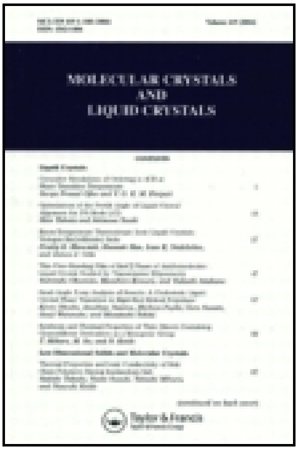

Molecular Crystals and Liquid Crystals
Publication details, including instructions for authors and subscription information:
http://www.tandfonline.com/loi/gmcl16

Chlorophyll-Liquid Crystal Electrodes for Photoenergy Conversion Modeled on Photosynthesis

Masuo Aizawa [a] [b] , Junichi Yoshitake [a] & Shuichi Suzuki [a]
[a] Research Laboratory of Resources Utilization, Tokyo Institute of Technology, Nagatsuta-cho, Midori-ku, Yokohama, 227, Japan
[b] Institute of Materials Science, University of Tsukuba, Sakura-mura, Ibaraki, 305, Japan

Version of record first published: 14 Oct 2011.

To cite this article: Masuo Aizawa , Junichi Yoshitake & Shuichi Suzuki (1981): Chlorophyll-Liquid Crystal Electrodes for Photoenergy Conversion Modeled on Photosynthesis, Molecular Crystals and Liquid Crystals, 70:1, 129-144

To link to this article: http://dx.doi.org/10.1080/00268948108073585

Mol. Cryst. Liq. Cryst., 1981, Vol. 70, pp. 129–144
0026-8941/81/7001-0129 $06.50/0

Chlorophyll-Liquid Crystal Electrodes for Photoenergy Conversion Modeled on Photosynthesis†

MASUO AIZAWA‡, JUNICHI YOSHITAKE AND SHUICHI SUZUKI

Research Laboratory of Resources Utilization, Tokyo Institute of Technology, Nagatsuta-cho, Midori-ku, Yokohama 227, Japan

(*Received August 22, 1980*)

Photoexcitable electrodes were prepared by coating a platinum plate with a membrane of chlorophyll and such a nematic liquid crystal as *N*-(*p*′-methoxybenzylidene)-*p*-butylaniline (MBBA) and 4′-heptyl-4-cyanobiphenyl (HCB). The incorporation of a liquid crystal considerably enhanced the electrode photoresponse. The photoelectrochemical properties of a chlorophyll-liquid crystal electrode depended on the metal species of the chlorophyll porphyrin. A MgChl-liquid crystal electrode behaved as a photocathode, in contrast a MnChl-liquid crystal electrode showed the photoanodic properties. The cathodic photocurrent of the MgChl-MBBA was attributed to the photoelectrochemical hydrogen evolution. On the other hand oxygen evolution was enhanced on illumination at the MnChl-HCB electrode. A photoelectrochemical cell was constructed by assembling the MgChl-MBBA and the MnChl-HCB electrodes.

A novel chlorophyll derivative, Ru chlorophyll (RuChl), was prepared and incorporated in a chlorophyll-liquid crystal electrode. A RuChl-MBBA electrode showed excellent performance as a photocathode.

The roles of the liquid crystals have been elucidated.

INTRODUCTION

Biomimetic photoenergy conversion systems have gained an increasing interest in relation to solar energy conversion. The thylakoid membrane involved in the chloroplast of green leaves is a current target to which many scientists have tried to approach. One of the approaches is to make a photoexcitable electrode modeled on the primary photosynthetic process

---

†Presented at the Eighth International Liquid Crystal Conference, Kyoto, July 1980.

‡Present Address: Institute of Materials Science, University of Tsukuba, Sakura-mura, Ibaraki 305, Japan

occurred in the thylakoid membrane. A chlorophyll electrode is a metal or semiconductor electrode covered with a chlorophyll layer. The chlorophyll is excited on illumination to pump up an electron from the base electrode to the electrolyte or *vice versa.*

Various chlorophyll electrodes have been proposed. The conceptual scheme of each chlorophyll electrode is shown in Figure 1. Tribusch fixed chlorophyll molecules at random on the ZnO semiconductor surface to develop the photo-induced unidirectional current.[1] Takahashi reported that photocurrent markedly increased by the incorporation of either electron acceptor or donner in the chlorophyll layer, and that either photoocathode or photoanode was prepared in combination of chlorophyll with an electron acceptor and donner.[2–4] It was shown by Fong that the chlorophyll-$2H_2O$ adduct was effective on the photo-induced charge separation of a chlorophyll electrode.[5–7] Honda and his coworkers demonstrated a high quantum efficiency with a chlorophyll monolayer electrode.[8]

The authors have proposed that a chlorophyll-liquid crystal composite layer provides an enhanced photoexcitable electrode.[9–12] The liquid crystal is expected to make an alignment of chlorophyll molecules on the base electrode surface in the similar manner to the mesomorphic phospholipids in the thylakoid membrane. The present investigation aimed at elucidating the roles of the liquid crystal on the photoexcitation of chlorophyll, and at confirming the liquid crystal effects on the photoexcitation of chlorophyll derivatives such as Ru chlorophyll in which the Mg of chlorophyll was substituted by Ru.

EXPERIMENTAL

Materials

Chlorophyll a (Chl a or MgChl) was isolated from fresh spinach leaves according to Jacobs' method.[13] Spinach leaves were crushed in liquid N_2, which was followed by extraction with cooled acetone. After filtration with gauze, petroleum ether was added to the extract. Water was added if necessary. The acetone soluble carotenoids and proteins were isolated from the chlorophyll mixtures. After the repeated isolation of the carotenoids and proteins, the petroleum ether solution of chlorophyll were applied on a sucrose column. Elution was made with petroleum ether, petroleum ether-ethyl ether (90:10 v/v %), and then petroleum ether-*i*-propanol (99.5:0.5 v/v %) to isolate chlorophyll a. The preparation was assayed by thin layer chromatography [benzene-*t*-butanole (90:10 v/v %)].

Mn chlorophyll (MnChl) was obtained from Nippon Chlorophyll Co., Ltd. (Tokyo).

Ru chlorophyll (RuChl) was prepared from Chl a and dodecacarbonyl tri-

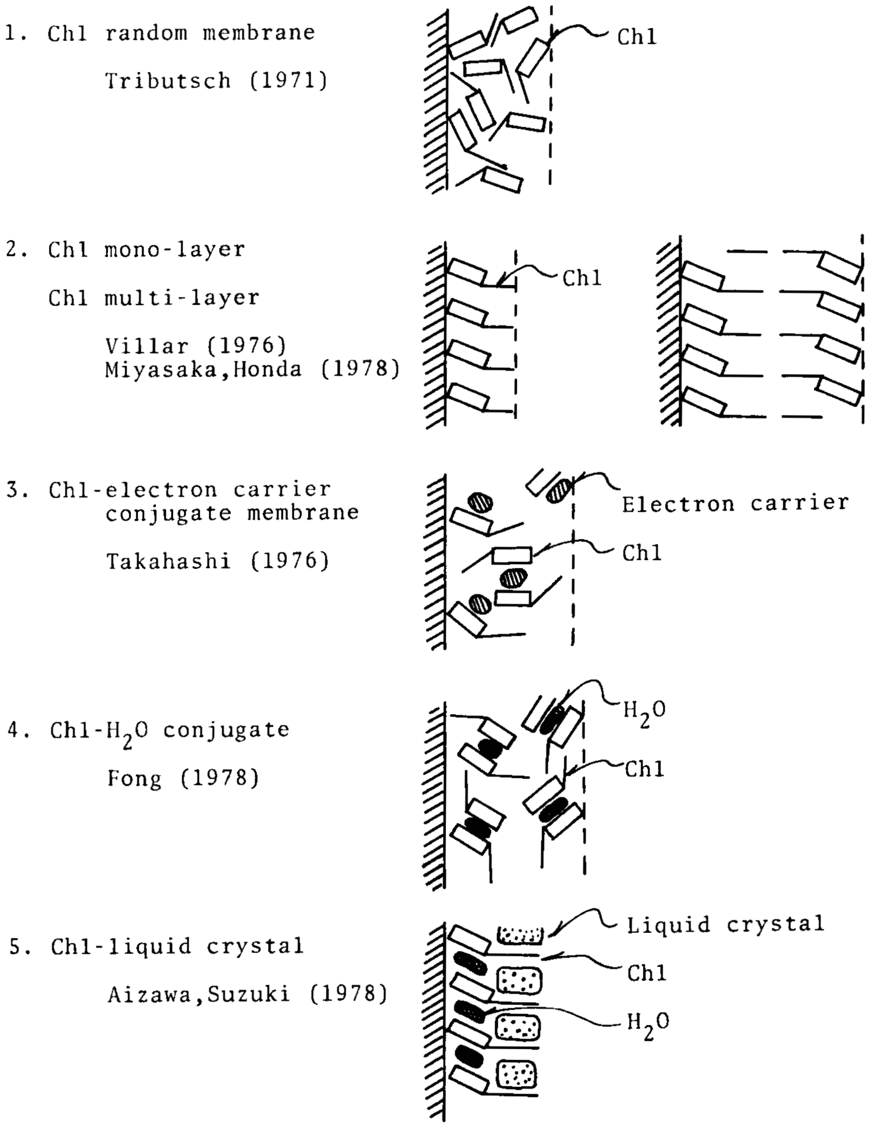

FIGURE 1 Conceptual schemes of various chlorophyll electrodes.

ruthenium (Ru$_3$(CO)$_{12}$). The stock solution of Chl a was evaporated. The Chl a (50 mg) was dissolved in hexane-ethyl ether (9:1). The solution was then mixed with 2% HCl. After vigorous mixing the aqueous layer was washed with 70% methanol twice and evaporated to yield 40 mg pheophytin a. The pheophytin a (40 mg) and Ru$_3$(CO)$_{12}$ (40 mg) were dissolved in benzene and refluxed under N_2 gas for 12 hr. The reaction mixture turned blue green. The product was applied on a thin layer chromatography plate and developed with benzene-*t*-butanol (1:9), which was followed by extraction with ethyl ether. The product was identified carbonyl-coordinated RuChl a (RuChlaCO). The RuChlaCO was then dissolved in pyridine and was allowed to stand under N_2 gas and light illumination at 70–80° C for 3 days. The product was found to be pyridine-carbonyl-coordinated RuChla [RuChlaPyr].

Preparation of chlorophyll-liquid crystal electrodes

Both chlorophyll and a liquid crystal were dissolved in a mixed solvent of petroleum ether and benzene (9:1). On the surface of a platinum plate (1×1 cm^2), 20 μl of the resulting solution was homogeneously spread and dried to yield a chlorophyll-liquid crystal electrode.

Photoelectrochemical characterization of chlorophyll-liquid crystal electrodes

Figure 2 shows the experimental setup for the photoelectrochemical characterization of chlorophyll-liquid crystal electrodes. A chlorophyll-liquid crystal electrode was immersed in a deoxygenated buffer solution in the dark. The electrode potential was measured with reference to a saturated calomel electrode (SCE). The electrode was illuminated by either monochromatic or white light. Although Figure 3 contains no temperature control system, the temperature was regulated within ±0.05° C. A water bath and a heat-cut filter were placed in front of the light source to absorb generated heat. The electrode potential was controlled with a potentiostat (Hokuto Denko Model PS-1000).

RESULTS AND DISCUSSION

Effects of liquid crystals on the photoresponse of the chlorophyll electrodes

Cholesteryl oleate (COL), *N*-(*p*′-methoxy benzylidene)-*p*-butyl aniline (MBBA), and 4′-heptyl-4-cyano biphenyl (HCB) were used to prepare the chlorophyll-liquid crystal electrodes. Each chlorophyll-liquid crystal electrode was in contact with an appropriate electrolyte solution in the dark. The electrode potential was determined with referring to SCE. When a steady dark potential was obtained, light was imposed on the chlorophyll electrode surface.

Figure 3 shows the photoresponses of several chlorophyll-liquid crystal electrodes to alternative illumination. A MnChl-HCB (1:9) electrode exhibited a negative-going potential shift when illuminated. The magnitude of

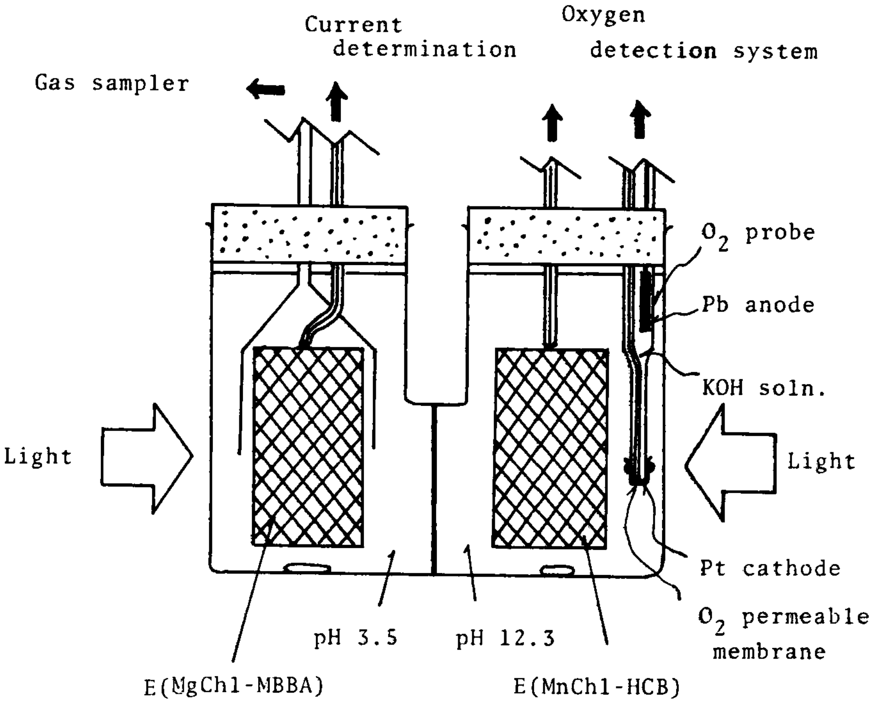

FIGURE 2 Experimental setup for the photoelectrochemical characterization of chlorophyll-liquid crystal electrodes. E(MgChl-MBBA) and E(MnChl-HCB): A MgChl-MBBA and MnChl-HCB electrodes.

the photoinduced potential shift was very small when the electrode was illuminated immediately after immersion in the electrolyte solution. The photoinduced potential shift was enhanced by consecutive illuminations, reaching a steady value. It should be noted that an electrode coated with a chlorophyll layer responded to light in an intensively retarded extent, and that excess incorporation of HCB depressed the photoresponse. The photoresponse was retarded in case MBBA was used in place of HCB. Unless HCB was incorporated, a very small photoinduced potential was obtained.

A MgChl-liquid crystal electrode showed the similar liquid crystal dependence, although the direction of potential shift was opposite to that of a MnChl-liquid crystal electrode as illustrated in Figure 4.

The photoresponse of a RuChl electrode was also enhanced by incorporation of a liquid crystal. The direction of the photoinduced potential shift changed depending on the coordinated species of RuChl. A carbonyl-coordinated RuChl electrode showed a negative-going photopotential shift in contrast with a positive-going shift with a pyridine-carbonyl-coordinated RuChl (RuChlPyr) electrode.

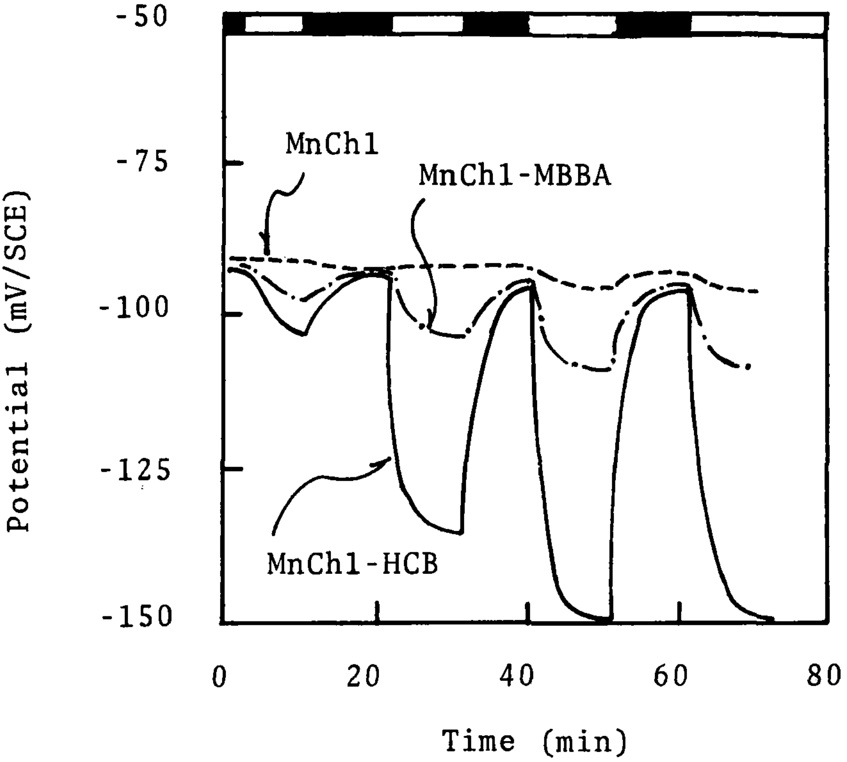

FIGURE 3 Photoinduced electrode potential changes of a MnChl, MnChl-MBBA, and MnChl-HCB electrodes.

Incorporation of a liquid crystal enhanced the magnitude of a photoinduced potential shift and resulted in a fast response to light. These effects of a liquid crystal should be highly evaluated in the development of a photoexcitable chlorophyll electrode.

The optimum molar ratio of a liquid crystal to chlorophyll was determined. A typical result is represented for MgChl-MBBA and MnChl-HCB electrodes in Figure 5. The photoinduced potential shift depended markedly on a molar ratio of a liquid crystal. The results indicated that a molar ratio of 3 was optimum.

Figure 6 shows a typical temperature dependence of the photoinduced potential shift derived from a chlorophyll-liquid crystal electrode. The photoinduced potential of a MnChl-MBBA electrode intensively increased with an increase in temperature between 23 and 45°C. Although the temperature effect was not so prominent, the photoinduced potential of an MnChl-HCB electrode increased in the range about 25–40°C. It is noted that the temperature effect appeared in the mesomorphic range of the incorporated liquid crystal. The mesomorphic state should play a key role on the enhancement of the electrode photoresponse.

States of chlorophyll immobilized in a liquid crystal membrane

To elucidate the roles of the liquid crystal on the enhancement of the electrode photoresponse, the molecular states of chlorophyll immobilized in a liquid crystal membrane was spectrophotometrically investigated. A MgChla-MBBA membrane was taken as an example, because the spectroscopic data of MgChla was available.

An ether solution of Chl a was homogeneously spread over a NaCl cell for IR measurement. After evaporation of ether, IR spectra were obtained with the cell. IR measurements were performed similarly with a Chl a-MBBA and a MBBA membranes.

Figure 7 shows absorption spectra for a MBBA, Chl a, and Chl a-MBBA (1:3 in molar ratio) in the IR region 1400–1800 cm^{-1}. Despite a very small

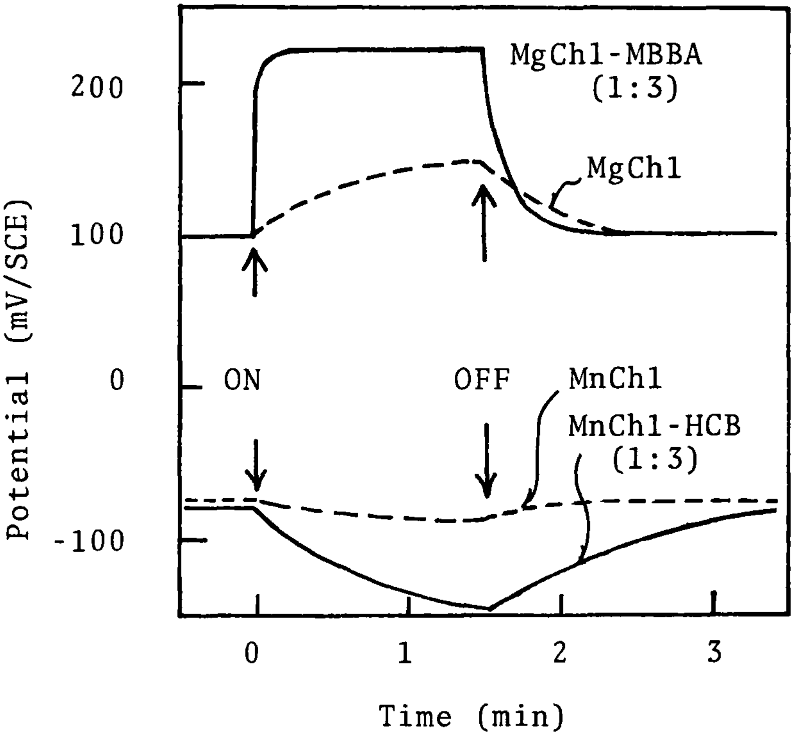

FIGURE 4 Effects of a liquid crystal on the photoinduced potential.

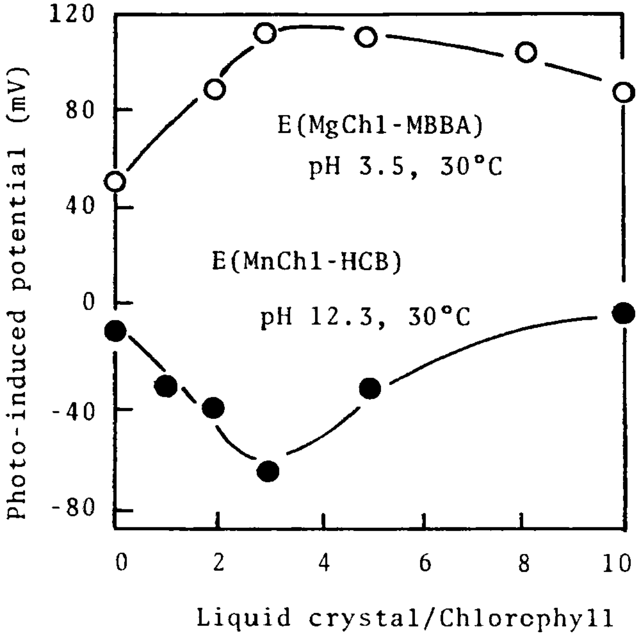

FIGURE 5 Effects of liquid crystal ratio on the photoinduced potential.

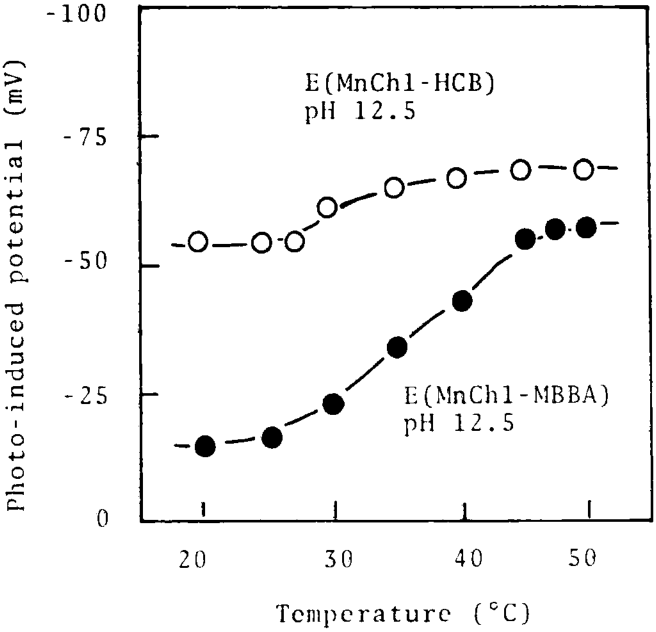

FIGURE 6 Temperature dependence of the photoinduced potential.

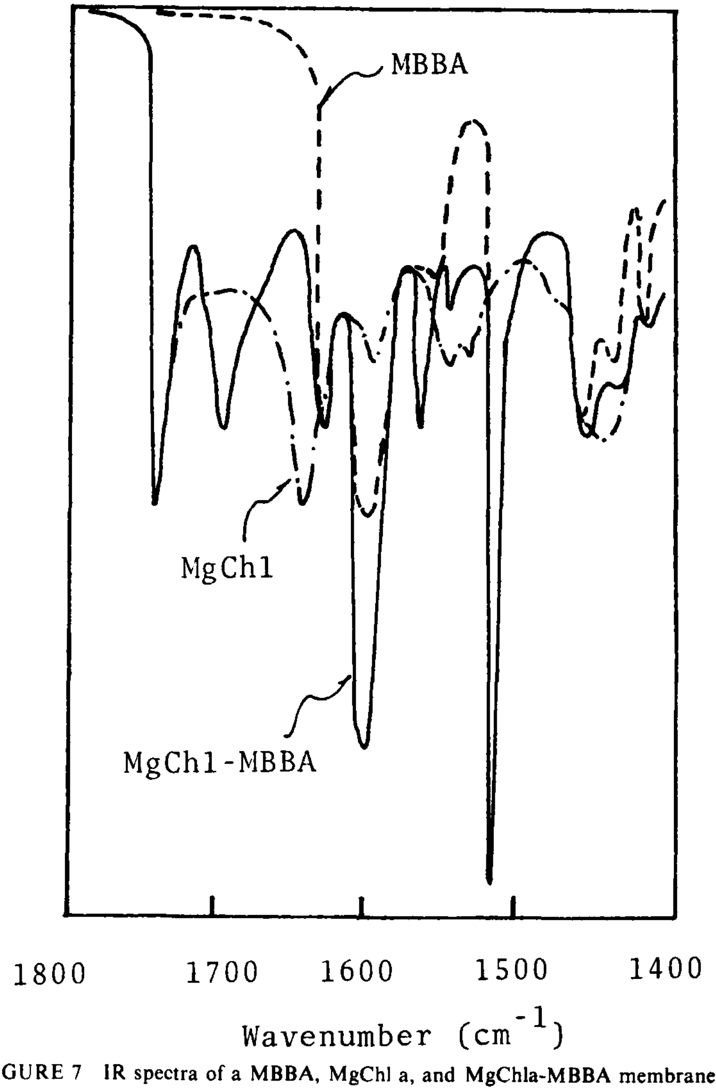

FIGURE 7 IR spectra of a MBBA, MgChl a, and MgChla-MBBA membranes.

absorption of a MBBA membrane at 1655 cm^{-1}, a Chl a membrane has a sharp peak at 1655 cm^{-1}, which is attributed to the intermolecular interaction between the C-9 keto C=O and the Mg of another porphyrin ring. In contrast the incorporation of MBBA resulted in disappearance of the peak at 1655 cm^{-1}. A new peak appeared at 1703 cm^{-1}, which was attributed to the free C-9 keto C=O. The peak shift is interpreted by the cleavage of the chlorophyll intermolecular interaction due to the penetration of MBBA. One of the liquid crystal role is considered to decouple the chlorophyll intermolecular interaction.

The 1703 cm^{-1} peak height, a measure of the free C-9 keto C=O, increased with an increase in MBBA molar ratio, reaching a saturated value at a MBBA molar ratio of 3. Figure 8 shows the relationship between the 1703 cm^{-1} peak height and the MBBA molar ratio of a Chla-MBBA membrane. The chlorophyll intermolecular interaction was cleaved by incorporating MBBA at a ratio of 3. It is a coincidence that the molecular length of MBBA is approximately one third of the chlorophyll phytol chain.

The IR spectra of a MgChl-COL, MgChl-HCB and MgChl-MBBA are comparatively illustrated in Figure 9. All chlorophyll-liquid crystal membranes were prepared at a molar ratio of chlorophyll:liquid crystal = 1:3. The 1703 cm^{-1} peak height is a measure to estimate the effects on the decoupling of the chlorophyll intermolecular interaction. Of these three liquid crystals, MBBA was found to decouple most effectively the chlorophyll intermolecular interaction. As stated, MBBA enhanced most prominently the electrode

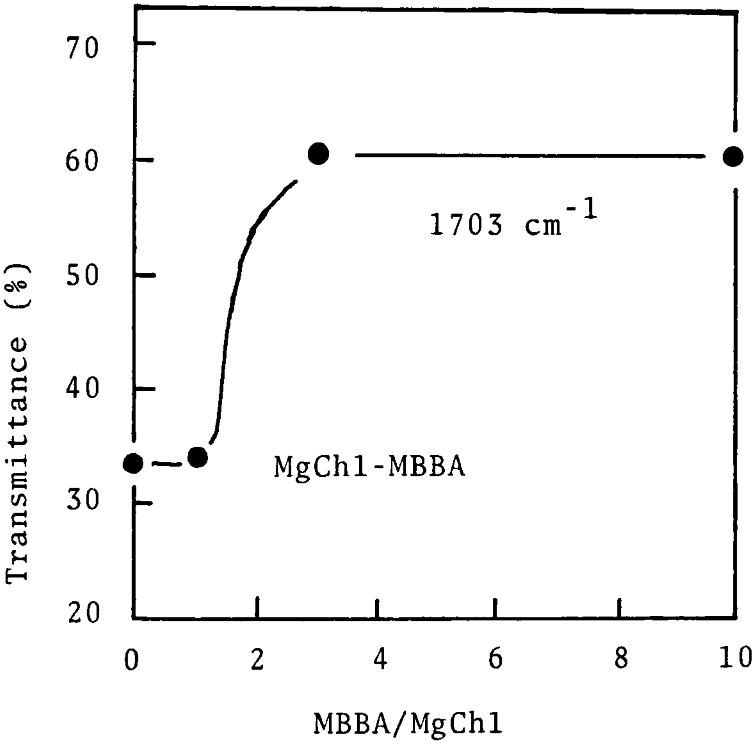

FIGURE 8 The 1703 cm^{-1} peak height at various MBBA ratios of the MgChl-MBBA membrane.

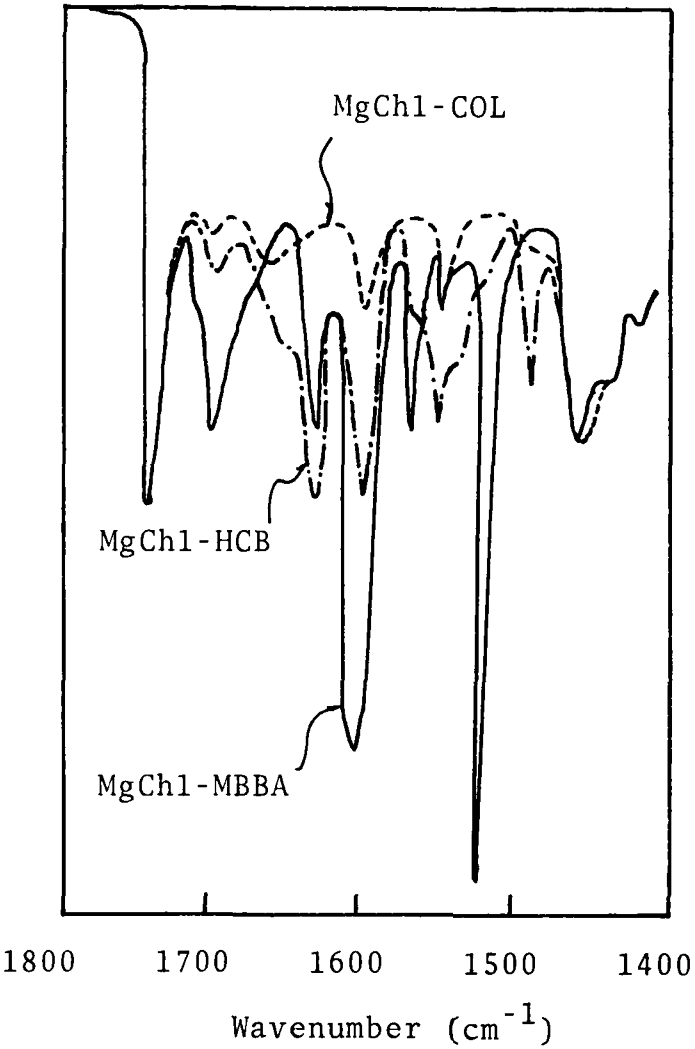

FIGURE 9 IR spectra of various MgChl-liquid crystal membranes.

photoresponse. The decoupling of the chlorophyll intermolecular interaction seems to be closely related with the effective photoresponse of chlorophyll electrodes.

Figure 10 suggests the formation of chlorophyll-water adduct in the MgChl-MBBA membrane when the membrane is in contact with water. Chl a absorbs at 663.0 nm when dissolved in 80% acetone, which is attributed to the monomeric state of chlorophyll. A chlorophyll a membrane, formed on a quartz plate, exhibits a 667.5 nm peak in dry state. When the membrane was in

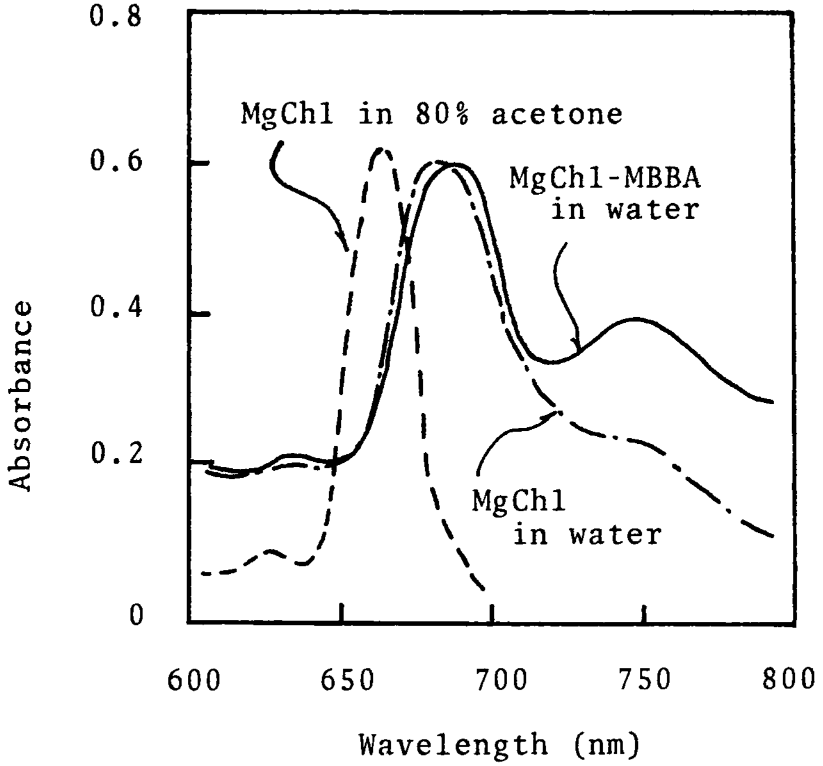

FIGURE 10 Absorption spectra of a MgChl-MBBA membrane in contact with water.

contact with water, a broad peak appeared at 740–750 nm. A Chl a-MBBA membrane was formed similarly on a quartz plate at a varied MBBA molar ratio. All the Chla-MBBA membranes (Chla:MBBA = 1:1, 1:3, and 1:10) showed a peak at 683.0 nm in dry state. As shown in Figure 10, the 740–750 nm peak appeared when the membrane was in contact with water.

Although the stoichiometry has not been settled,[14,15] the 740-750 nm peak is attributed to a chlorophyll-water adduct. Figure 10 indicates that a MgChl-MBBA membrane contains a chlorophyll-water adduct. MBBA decouples the chlorophyll intermolecular interaction so effectively that water may bridge the porphyrin rings of adjacent chlorophyll molecules.

A MBBA molar ratio of 3 was optimum, which could be interpreted as follows. The molar length of MBBA is approximately one third of the phytol chain length. Three MBBA molecules are thought to make a line between the two phytol chains of adjacent chlorophylls so that water molecules might penetrate into the interporphyrin space. In addition, MBBA may be ordered due to sharp potential gradient at the electrode surface; thus the molecular alignment is considered to contribute to the effective charge separation and transfer of chlorophyll molecules in photoexcitation.

Photocurrent of chlorophyll-liquid crystal electrodes

The photocurrent characteristics are presented for a MgChl-MBBA (MgChl:MBBA = 1:3 in molar ratio, 1.4×10^{-8} mole MgChl/cm^2) and a MnChl-HCB (MnChl:HCB = 1:3 in molar ratio, 1.4×10^{-8} mole MnChl/cm$_2$) electrodes in Figure 12. The MgChl-MBBA electrode was set in a cell illustrated in Figure 2. The pH of the electrolyte was adjusted at 3.5 by M/30 acetate buffer. The temperature was regulated at 30 ± 0.5°C. The electrode potential was controlled with a potentiostat in the dark. The electrode was then illuminated. Steady current was recorded in the dark and on illumination. The differential current between these two states was determined as the photoinduced current. The electrode potential was changed stepwise so as to obtain a photoinduced current *vs* controlled electrode potential curve. The MgChl-MBBA electrode derived the cathodic photo-

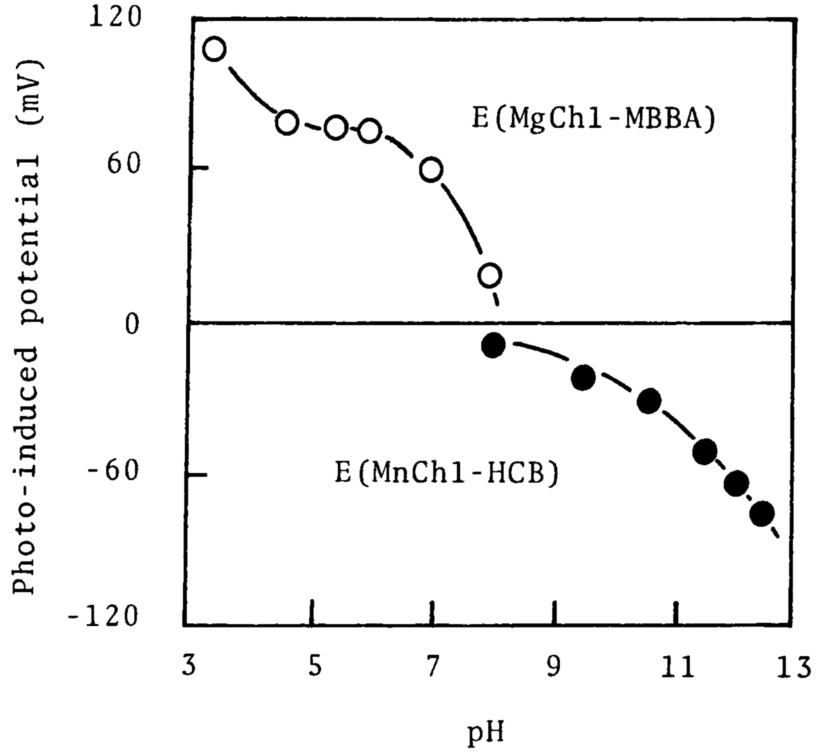

FIGURE 11 The pH dependency of the photoinduced potential.

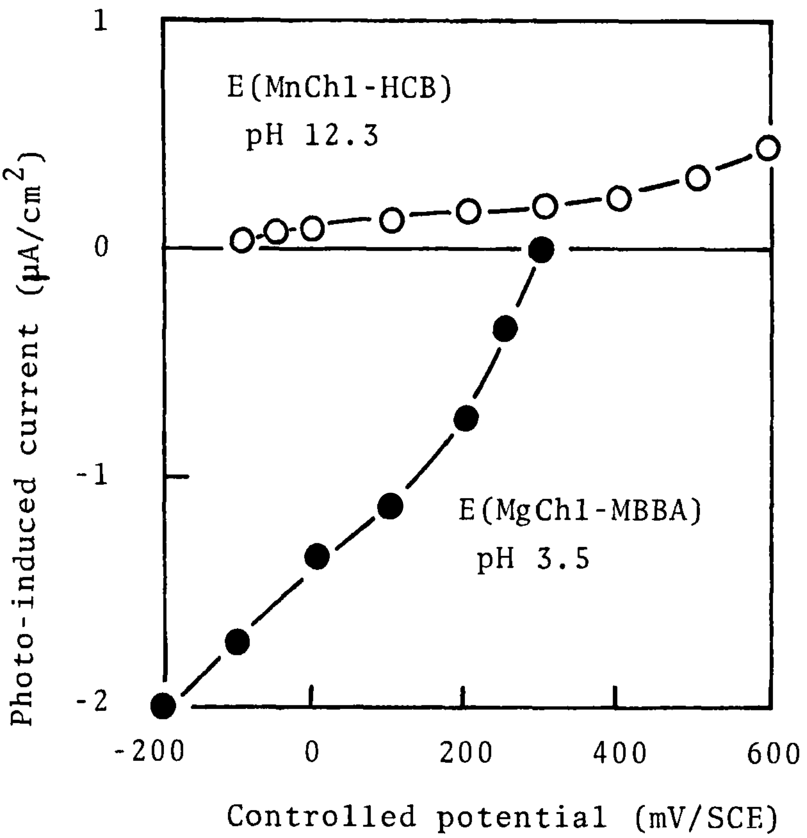

FIGURE 12 Photoinduced current *vs* electrode potential curves of the MgChl-MBBA and MnChl-HCB electrodes.

induced current below 280 mV/SCE as shown in Figure 12. The MgChl-MBBA electrode behaved as a photocathode under the conditions.

In contrast, the MnChl-HCB electrode gave the photoanodic characteristics. Above −90 mv/SCE, the anodic current of the MnChl-HCB electrode increased on illumination at pH12.3 of M/30 phosphate buffer.

It should be noted that the photoelectrochemical properties of a chlorophyll-liquid crystal electrode depend extremely on the metal species of the chlorophyll porphyrin. Of various metalochlorophylls such as FeChl, ZnChl, NiChl, CuChl, and MnChl, only MnChl showed the photoanodic properties.

The photoelectrochemical reactions of the MgChl-MBBA and the MnChl-HCB electrodes were investigated. The electrolyte was preliminarily bubbled with N_2 gas to eliminate dissolved oxygen and hydrogen. The electrode potential of the MgChl-MBBA electrode was controlled at an appropriate potential on illumination. The photoelectrochemical reaction was continued at pH 3.5 for 2 hr. The gas evolved from the MgChl-MBBA electrode was collected in a gas sampler and was assayed by gas chromatography. A gas chromatograph (Shimadzu Model GC-6AM) with a digital integrator (Shimadzu Model ITG-4A) was used with a column (3 mm I.D. × 2 m) loaded with Molecular Sieve 5A and heated at 42°C. Argon gas was used as the carrier gas. The gas was analyzed by the thermal conducting method. The amount of hydrogen gas was determined at various electrode potentials. The hydrogen gas evolution from the MgChl-MBBA electrode was considerably enhanced by illumination. The similar experiment was performed with the MnChl-HCB electrode. Oxygen gas evolved from the MnChl-HCB electrode was directly monitored with a Clark-type dissolved oxygen probe which was set in the vicinity of the electrode. The dissolved oxygen concentration increased in parallel with an increase of photocurrent.

In conclusion the photolysis of water was catalyzed by the MgChl-MBBA and the MnChl-HCB electrodes.

An improved chlorophyll-liquid crystal electrode

A photoelectrochemical cell was constructed by assembling the MgChl-MBBA and the MnChl-HCB electrodes. However, the photocurrent of the cell was small as estimated from the photoelectrochemical properties of these electrodes presented in Figure 12. A new chlorophyll electrode was developed using RuChlPyr. A RuChl-MBBA electrode was prepared in the similar manner at a molar ratio of RuChl:MBBA = 1:3. A RuChlPyr-MBBA electrode showed the cathodic photocurrent as presented in Figure 13. The photocurrent increased appreciably as compared with that of the MgChl-MBBA electrode. Furthermore, the RuChl-MBBA electrode showed such an improved performance at a neutral pH, while the maximum photocurrent of the MgChl-MBBA electrode was obtained at pH3.5.

CONCLUSIONS

Incorporation of a liquid crystal was effective on the enhancement of the chlorophyll electrode photoresponse. A liquid crystal is considered to enable chlorophyll to form a chlorophyll-water adduct and to make an ordered alignment on the metal surface. Various chlorophyll-liquid crystal electrodes including a MgChl-MBBA, MnChl-HCB, and RuChl-MBBA electrodes were photoelectrochemically characterized. A RuChl-MBBA electrode appears promising in assembling an electrochemical photocell.

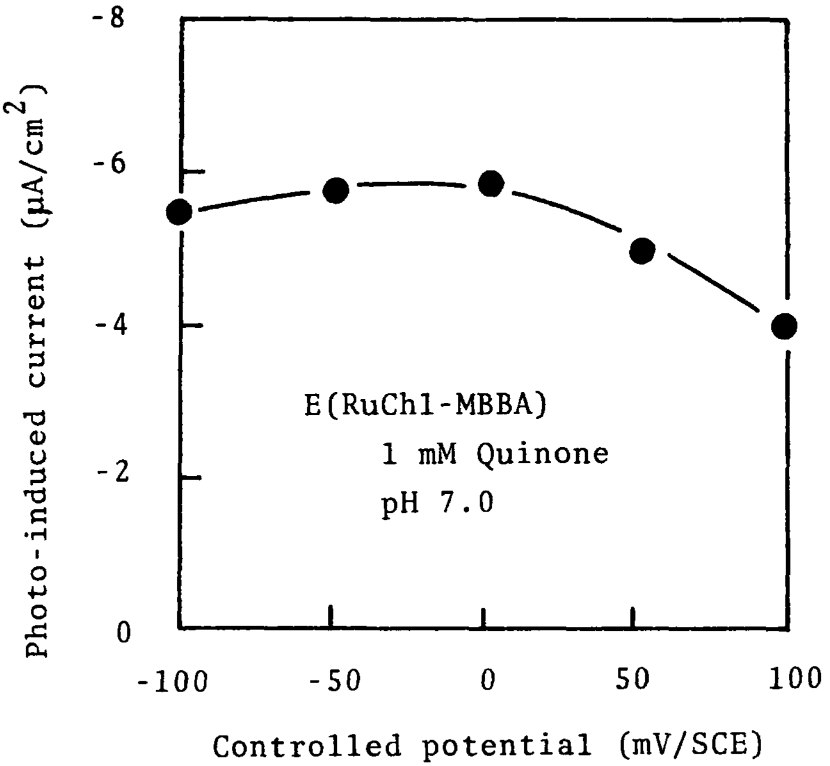

FIGURE 13 The photocurrent characteristics of the RuChl-MBBA electrode.

References

1. H. Tribusch and M. Calvin, *Photochem. Photobiol.*, **14**, 95 (1971).
2. F. Takahashi and R. Kikuchi, *Biochim. Biophys. Acta*, **430**, 490 (1976).
3. F. Takahashi and R. Kikuchi, *Bull. Chem. Soc. Japan.*
4. F. Takahashi, M. Aizawa, R. Kikuchi and S. Suzuki, *Electrochim. Acta*, **22**, 289 (1977).
5. F. K. Fong and L. Galloway, *J. Am. Chem. Soc.*, **100**, 3594 (1978).
6. F. K. Fong and N. Winograd, *J. Am. Chem. Soc.*, **98** 2287 (1976).
7. L. M. Fetterman, L. Galloway, N. Winograd and F. K. Fong, *J. Am. Chem. Soc.*, **99** 653 (1977).
8. T. Miyasaka, T. Watanabe, A. Fujishima and K. Honda, *J. Am. Chem. Soc.*, **100** 6657 (1978).
9. M. Aizawa, N. Suzuki, F. Takahashi and S. Suzuki, *J. Solid-Phase Biochem.*, **2** 111 (1977).
10. M. Aizawa, N. Suzuki, M. Hirano and S. Suzuki, *Electrochim. Acta*, **23** 1061 (1978).
11. M. Aizawa, M. Hirano and S. Suzuki, *Electrochim. Acta*, **23** 1185 (1978).
12. M. Aizawa, M. Hirano and S. Suzuki, *Electrochim. Acta*, **24** 89 (1978); *J. Membrane Sci.*, **4** 251 (1978).
13. E. E. Jacobs, A. E. Vatter and A. S. Holt, *Arch. Biochem. Biophys*, **53** 228 (1954).
14. J. G. Brace, F. K. Fong, D. H. Karweik, V. J. Koester, A. Shepard and N. Winograd, *J. Am. Chem. Soc.*, **100** 5203 (1978).
15. L. L. Shipman and J. J. Katz, *J. Phys. Chem.*, **81** 577 (1977).